Vertical stratification and air-sea CO_2 fluxes in the Patagonian shelf

Alejandro A. Bianchi,[1,2] Laura Bianucci,[2] Alberto R. Piola,[1,2] Diana Ruiz Pino,[3] Irene Schloss,[4,5] Alain Poisson,[3] and Carlos F. Balestrini[1]

Received 14 May 2004; revised 9 March 2005; accepted 24 March 2005; published 7 July 2005.

[1] The thermohaline structure across the tidal fronts of the continental shelf off Patagonia is analyzed using historical and recent summer hydrographic sections. The near-summer tidal front location is determined on the basis of the magnitude of vertical stratification of the water column as measured by the Simpson parameter. Sea surface and air CO_2 partial pressures based on data from eleven transects collected in summer and fall from 2000 to 2004 are used to estimate CO_2 fluxes over the shelf. The near-shore waters are a source of CO_2 to the atmosphere while the midshelf region is a CO_2 sink. The transition between source and sink regions closely follows the location of tidal fronts, suggesting a link between vertical stratification of the water column and the regional CO_2 balance. The highest surface values of Chl *a* are associated with the strongest CO_2 sinks. The colocation of lowest CO_2 partial pressure (pCO_2) and highest Chl *a* suggests that phytoplankton blooms on the stratified side of the fronts draw the ocean's CO_2 to very low levels. The mean shelf sea-air difference in pCO_2 (ΔpCO_2) is -24 μatm and rises to -29 μatm if the shelf break front is included. Peaks in ΔpCO_2 of -110 μatm, among the highest observed in the global ocean, are observed. The estimated summer mean CO_2 flux over the shelf is -4.4 mmol m^{-2} d^{-1} and rises to -5.7 mmol m^{-2} d^{-1} when the shelf break area is taken into account. Thus, during the warm season the shelf off Patagonia is a significant atmospheric CO_2 sink.

Citation: Bianchi, A. A., L. Bianucci, A. R. Piola, D. R. Pino, I. Schloss, A. Poisson, and C. F. Balestrini (2005), Vertical stratification and air-sea CO_2 fluxes in the Patagonian shelf, *J. Geophys. Res.*, *110*, C07003, doi:10.1029/2004JC002488.

1. Introduction

1.1. Study Area: Background

[2] The area covered by the Argentine shelf is close to 1,000,000 km^2. It is characterized by a smooth slope and scarce relief features [*Parker et al.*, 1997]. The shelf broadens from north to south, ranging from 170 km at 38°S to more than 600 km south of 50°S. The main source of the shelf water masses is the subantarctic water flowing from the northern Drake Passage, through the Cape Horn Current [*Hart*, 1946] between the Atlantic coast and the Malvinas Islands, and the Malvinas Current in the eastern border of the shelf [*Bianchi et al.*, 1982]. The fresh water sources of the shelf are the small continental discharge and the low-salinity water outflowing from the Magellan Strait. The latter is due to high precipitation in the South Pacific, close to the west coast of Tierra del Fuego, and the melting of continental ice [*Lusquiños*, 1971a, 1971b; *Lusquiños and Valdés*, 1971; *Piola and Rivas*, 1997]. The present study is limited to the area south of 39°S and consequently south of the region influenced by the input and variability of the Plata river. In addition, the evaporation-precipitation imbalance locally affects the salinity of some areas.

[3] Because seasonal variability precludes the utilization of temperature to classify the water masses, salinity is frequently used for this purpose. Four water masses can be defined according to salinity (Figure 1): Malvinas water (>33.8), coastal water (low salinity, <33.4), shelf water or midshelf water, ranging from 33.4 to 33.8, and a high-salinity coastal water close to the San Matías and Nuevo Gulfs, where the low-salinity tongue arising from the Magellan Strait turns offshore [*Bianchi et al.*, 1982; *Guerrero and Piola*, 1997]. The surface salinity in the San Matías Gulf (SMG) is higher than 34.0 because of enhanced evaporation [*Scasso and Piola*, 1988]. The SMG positive thermal anomaly relative to the adjacent shelf waters [*Krepper and Bianchi*, 1982] is probably due to a greater residence time in the gulf [*Piola and Scasso*, 1988; *Rivas and Beier*, 1990].

[4] Abrupt changes in the water properties define ocean fronts. In the Argentine shelf, these fronts are the shelf break front, between the Malvinas waters and midshelf waters [*Martos and Piccolo*, 1988; *Carreto et al.*, 1995] and tidal fronts [*Carreto et al.*, 1986; *Glorioso*, 1987], that develop in the warm season between vertically homogeneous coastal waters and stratified midshelf waters. Both the shelf break

[1]Departamento Oceanografía, Servicio de Hidrografía Naval, Buenos Aires, Argentina.
[2]Departamento Ciencias de la Atmósfera y los Océanos, FCEN, Universidad de Buenos Aires, Ciudad Universitaria, Buenos Aires, Argentina.
[3]Laboratoire de Biogéochimie et Chimie Marines, Université Pierre et Marie Curie, Paris, France.
[4]Instituto Antártico Argentino, Buenos Aires, Argentina.
[5]Consejo Nacional de Investigaciones Científicas y Técnicas, Buenos Aires, Argentina.

0148-0227/05/2004JC002488

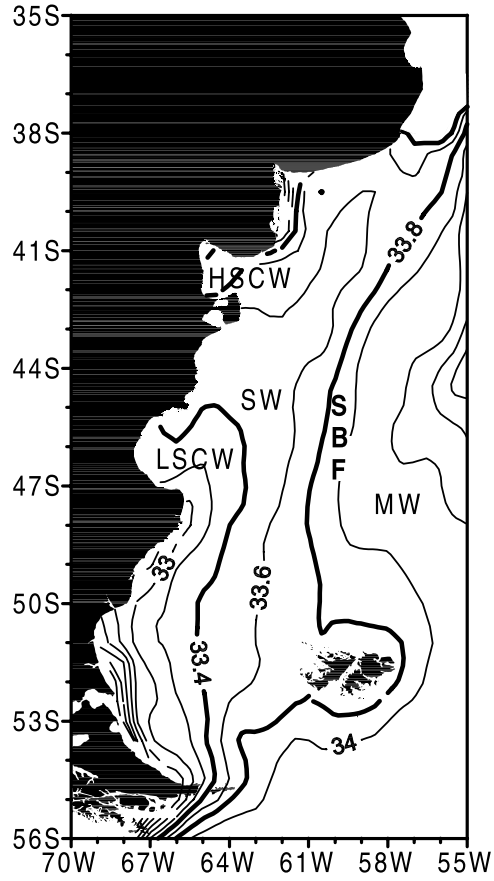

Figure 1. Climatological sea surface salinity horizontal distribution. The isohalines that separate water masses are shown (33.4 and 33.8). Abbreviations are as follows: low-salinity coastal water (LSCW), high-salinity coastal water (HSCW), shelf water (SW), Malvinas water (MW) and shelf break front (SBF).

front and the tidal fronts are the borders that delimit the above defined water masses (Figure 1).

[5] South of 41°S, the shelf width is close to one quarter of the semidiurnal tide wavelength leading to favorable conditions for resonance [*Piola and Rivas*, 1997]. The tidal amplitude in the Patagonian shelf is one of the highest in the world ocean [*Kantha et al.*, 1995], and tidal currents are very energetic. Consequently, by vertically mixing the coastal waters, the tidal current bottom friction is a key mechanism in the generation of the tidal fronts. These processes can generate upwelling regions in the Patagonian shelf [*Simpson and Hunter*, 1974; *Bakun and Parrish*, 1991]. Using numerical models, *Glorioso and Flather* [1997] identified regions where the tidal energy dissipation is likely to produce these conditions, i.e., offshore Valdés Peninsula (VP), Cabo Blanco (CB), and the region between 50°S and De los Estados Islands. *Palma et al.* [2004] used a high-resolution barotropic model to determine the location of the main frontal systems of the Patagonian shelf and found a good correspondence with summer sea surface temperature (SST) gradients. Their results are similar to those of *Glorioso and Flather* [1997], showing the most intense fronts near of VP, north of SMG and off Grande Bay (GB). The analysis of 11 years of satellite-derived SST shows that the tidal fronts are persistent throughout the year, except during winter [*Bava et al.*, 2002].

[6] Generally, front creation is linked to two physical mechanisms [*Hoskins and Bretherton*, 1972]: (1) differential advection, either convergences or shear deformation in the horizontal flow, or (2) differential vertical mixing. In coastal regions, tidal fronts are a clear example of the last case. The biological response to fronts at every trophic level involves the extreme sensitivity of the ocean ecosystem to vertical motion [*Olson*, 2002]. Thus air-sea CO_2 fluxes at both sides of tidal fronts are related to the response of phytoplankton to the frontal environment.

1.2. CO_2 Balance

[7] The world ocean plays a major role in the global carbon cycle budget. Carbon in the oceans is unevenly distributed because of complex circulation patterns and biogeochemical cycles, neither of which is completely understood. In addition to circulation patterns, part of the CO_2 is absorbed by the biota, both on land and in the ocean. The ocean CO_2 concentration is related to the biology of the organisms through photosynthesis, respiration, and calcification. The oceans are estimated to hold 38,000 gigatons (GT = 10^{12} kg) of carbon, which is 50 times the amount contained in the atmosphere. The annual air-sea exchange is 15 times larger than the amount produced by the burning of fossil fuels, deforestation, and other human activities [*Williams*, 1990]. The magnitude and direction of CO_2 annual net uptake flux by the global ocean is governed by the sea surface and air partial pressure of carbon dioxide (pCO_2) differences and the wind speed. However, because pCO_2 spatial and seasonal variations in the ocean surface are much larger than in the atmosphere, the oceanic pCO_2 is the main regulator of the sea-air transfer flux. The ocean surface pCO_2 varies about 25% above and below the current atmospheric pCO_2 level of approximately 360 μatm [*Takahashi et al.*, 2002]. Small regional sea areas can produce intense sequestration or releasing of CO_2. Because continental shelves are active regions in biological production, they are believed to play a significant role in the global CO_2 balance. Spring-summer observations from the Bering Sea shelf revealed variability in CO_2 fluxes associated with biological processes, insolation and vertical mixing [*Codispoti et al.*, 1986]. Recently, several authors have studied air-sea CO_2 fluxes in continental shelves and marginal seas [e.g., *Tsunogai et al.*, 1999; *Frankignoulle and Borges*, 2001; *Sarma*, 2003; *Thomas et al.*, 2004; *Hales et al.*, 2005]. The South Atlantic Ocean between 14°S and 50°S is believed to be a sink of about −0.3 to −0.6 GT C yr^{-1} [*Takahashi et al.*, 2002]. On the basis of the research in the East China Sea, *Tsunogai et al.* [1999] proposed that the cross-shelf circulation enhances the absorption of atmospheric CO_2 over the shelf and transfers these waters to subsurface layers in the open ocean. If the world continental shelf zone absorbed the atmospheric CO_2 at the rate observed in the East China Sea, this mechanism would account for a net oceanic uptake of CO_2 of 1 GT C yr^{-1}. Extrapolating the CO_2 uptake of the North Sea to the global scale, *Thomas et al.* [2004] estimated that 0.4 GT C yr^{-1} would sink in the coastal seas. However, more field data are needed to constrain a worldwide extrapolation, because

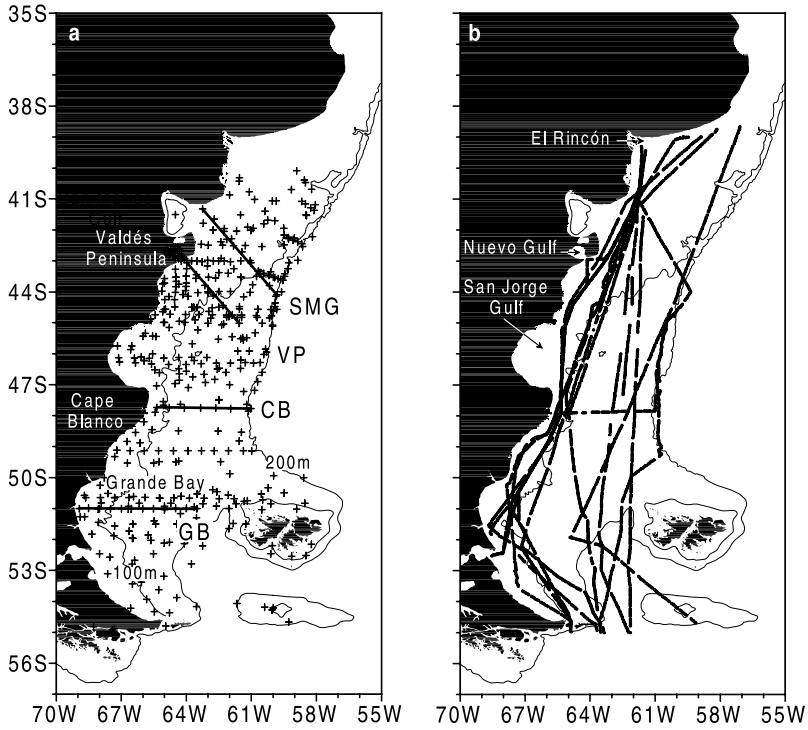

Figure 2. (a) Historical summer hydrographic data. The locations of the four transects used for the characterization of the fronts are shown: San Matías Gulf (SMG), Valdés Peninsula (VP), Cape Blanco (CB), and Grande Bay (GB). (b) Tracks performed by Icebreaker *Almirante Irizar* during ARGAU cruises from 2000 to 2004.

tropical continental shelves and river plumes could act as sources of atmospheric CO_2 [*Frankignoulle and Borges*, 2001]. Thus it is useful to evaluate the role of the large Patagonian shelf on the global CO_2 balance of shallow seas.

[8] Large marine ecosystems (LME) are oceanic regions encompassing coastal areas to the seaward boundaries of continental shelves and are characterized by their primary productivity, hydrography, trophically dependent populations, and bathymetry [*Bakun*, 1993]. On a global scale, 64 LME have been identified, and they produce 95% of the world's annual marine fisheries. On the basis of global primary production estimates from satellite images, the Patagonian continental shelf (LME 14) has been classified as a LME Class 1 (primary productivity >300 gC m^{-2} yr^{-1} [*Behrenfeld and Falkowski*, 1997]). Improving our knowledge of the relationship between vertical stratification, nutrient availability, and phytoplankton abundance is crucial for the living resources management. It is well known that the distribution of fisheries is tied to frontal regions and their variability [*Bisbal*, 1995]. Economic and ecologically important species such as anchovy, Patagonian scallop, and atherinids take advantage of the Patagonian tidal zone [*Acha et al.*, 2004; *Quintana and Yorio*, 1997].

[9] A cooperative research program named ARGAU (Programme de Coopération avec la Argentine pour l'étude de l'océan Atlantique Austral) between the Laboratoire de Biogéochemie et Chemie Marines (LBCM) at the Université Pierre et Marie Curie in Paris, France, the Instituto Antártico Argentino (IAA) and the Servicio de Hidrografía Naval (SHN), both from Argentina, was launched in 2000. One specific objective is to study the relation between frontal regions and air-sea CO_2 fluxes [*Piola et al.*, 2001].

[10] In this work, we discuss the relation between frontal regions, vertical stratification, phytoplankton biomass (expressed as chlorophyll *a*), and air-sea CO_2 fluxes. In section 2 the data and methods are described. In section 3 the characterization of the tidal fronts in the Patagonian shelf and the relations between environmental features with the shelf CO_2 budget are presented. Finally, the results are discussed in section 4. The role of planktonic community production and respiration processes in the regulation of CO_2 fluxes will be subject of future works.

2. Data and Methods

[11] Two different sets of data were used for the present study: historical hydrographic data (Figure 2a) from the Argentine Oceanographic Data Center (CEADO) and data from the ARGAU cruises (Figure 2b and Table 1). In addition, the Instituto Nacional de Investigación y Desarrollo Pesquero (INIDEP) furnished recent data from 13 stations in the area of GB. The CEADO database holds 433 stations collected during austral summer (January, February, and March) from 1927 to 1996. Vertical sections and horizontal distributions of temperature, salinity, and density were used to characterize frontal systems in four selected regions. To determine the location of ocean fronts, the Simpson parameter was estimated [*Simpson*, 1981]. The Simpson parameter, a measure of the mechanical work required to vertically mix the water column, is defined as

$$\Phi = \frac{g}{h} \int_{-h}^{0} (\rho - \rho_0) \cdot z \cdot dz,$$

Table 1. Details of the ARGAU Transects Used[a]

Cruise	Transects	Dates
ARGAU-0	1	24–25 March 2000
ARGAU-0	2	27–30 March 2000
ARGAU-1	3	24–27 January 2001
ARGAU-1	4	19–21 February 2001
ARGAU-1	5	5–8 April 2001
ARGAU-2	6	31 January to 2 February 2002
ARGAU-2	7	23–26 March 2002
ARGAU-2	8	10–13 April 2002
ARGAU-2	9	3–5 May 2002
ARGAU-3	10	7–10 February 2003
ARGAU-3	11	15–18 May 2003
ARGAU-4	12	27 February to 1 March 2004
ARGAU-4	13	13–16 March 2004
ARGAU-4	14	14–17 April 2004

[a]Cruises were carried out aboard Icebreaker *Almirante Irizar*.

where g is the gravity, h is the depth, and ρ_0 is the mean density of the water column. Small values of Φ indicate poorly stratified waters while high values are associated with stratified waters.

[12] Near sea surface (9 m depth) temperature, salinity, fluorescence, and ocean and atmosphere pCO_2 were collected underway along 14 transects (Table 1). Data were averaged and recorded at 10 min intervals. The sampling system for pCO_2 in air and seawater and associated parameters was developed at LBCM [*Poisson et al.*, 1993]. The system uses an infrared technique described by *Takahashi* [1961] and *Copin-Montégut* [1985]. It consists of a flow-through equilibrator and an IR analyzer (SIEMENS, type Ultramat 5F). The analyzer was calibrated every 6 hours with three gas standards containing 270.0, 361.0, and 489.9 ppm mole fraction of CO_2. Atmospheric pCO_2 was also measured every 6 hours from an intake placed on the bow of the ship. Using temperature data obtained from high-accuracy sensors placed in the equilibrator and in the seawater intake, pCO_2 was corrected for warming effects. Water pCO_2 was also corrected for atmospheric pressure variations, drift, and moisture effects. Except when measurements are in a region of very high variability (e.g., subantarctic front), the standard deviation of water pCO_2 is lower than 0.3%, about 1 μatm [*Metzl et al.*, 1995]. The observed range of atmospheric pCO_2 is 11 μatm, while for the sea pCO_2 it is about 260 μatm. Therefore the oceanic pCO_2 is the driving factor in the computation of sea-air pCO_2 difference (ΔpCO_2). Chlorophyll *a* (Chl *a*) was determined from 1.5 to 2 liter samples taken every 3 hours from the same water source entering the pCO_2 system and GF/F filtered. The filters were stored in dark at −20°C, and their analysis was carried out 3 months later after adding 8 ml 90% acetone. The extracts were read in a Beckman DU 650 spectrophotometer. Calculations of pigment concentrations were done according to *Strickland and Parsons* [1972].

[13] To compute CO_2 fluxes, the effect of two variables must be taken into account: the wind and the CO_2 solubility in seawater (k_S). The coefficient of gas transfer velocity (k_W) is obtained as a cubic function of the wind, according to *Wanninkhof and McGillis* [1999] (hereinafter referred to as WMG99). The CO_2 fluxes were estimated as follows:

$$CO_2\ \text{Flux} = k_S \cdot k_W \cdot \Delta pCO_2,$$

where the solubility was computed according to *Copin-Montégut* [1996]. We also calculated the CO_2 fluxes using k_W based on a quadratic expression by *Wanninkhof* [1992] (hereinafter referred to as W92).

[14] Since only seven of the transects had in situ wind data, wind speed for the remaining transects was obtained from the QuikScat winds. The QuikScat wind data are available twice a day, with a resolution of 0.25° latitude × 0.25° longitude. The grid nodes recovered are those closest to the in situ observations. Cubic spline interpolation was performed to obtain wind data every 2 hours for each grid node. After interpolation, satellite wind data closest in time to the in situ data were selected. These data are located on the grid nodes over the ship transects. To fill spaces between two consecutive grid nodes over a transect, satellite data were linearly interpolated in space. For three transects where in situ wind data were available (transects 6, 7, and 9, see Table 1), the standard deviation of the QuikScat data versus ship wind data was in a range of 1.3 to 2.2 m s^{-1}. The propagation of this error on the CO_2 flux estimates leads to relative errors ranging from 20 to 50%.

3. Results

3.1. Fronts Characterization

[15] The vertical sections presented in this work are based on stations from transects of the project Pesquería [*Villanueva*, 1968]. The main characteristics of the studied fronts are presented in Table 2. Four transects were selected to characterize tidal fronts (Figure 2a): SMG, VP, CB, and GB. Though salinity was used to characterize the water masses, in summer and in a synoptic scale, the vertical sections show that temperature dominates the density field since both isotherms and isopycnals describe similar patterns (Figure 3). The density sections reveal the transition between well-mixed near-shore waters and midshelf stratified waters. The low-salinity tongue described in section 1.1 is evident in every transect but only appears to have a significant effect on the density structure in the near coastal region in the CB and GB section.

[16] Horizontal scales of the tidal fronts are not well defined because of the relatively large distance between stations. Analysis of thermal fronts from satellite SST data (NOAA-AVHRR Global Area Coverage, resolution 4.5 km × 4.5 km) indicates spatial scales of 36 km in VP and SMG fronts and 12 km to 32 km in CB front [*Bava et al.*, 2002].

[17] At SMG, VP, and GB the quasi-homogeneous waters on the western side of the front are warmer than the midshelf stratified region. This is due to the resolution of

Table 2. Thermohaline Characteristics of the San Matías Gulf (SMG), Valdés Peninsula (VP), Cabo Blanco (CB), and Grande Bay (GB) Fronts[a]

	Mixed Zone			Front Distance to the Coast, km	Maximum Stratification	
	T, °C	S	σ_t		$\Delta\sigma_t$	Depth, m
SMG	18.0	34.2	24.6	150	1.2	70
VP	16.0	33.6	24.7	50	1.2	75
CB	12.0	32.9	25.0	80	0.8	94
GB	11.2	32.9	25.1	16	0.4	92

[a]$\Delta\sigma_t$ values are the differences between surface and bottom data.

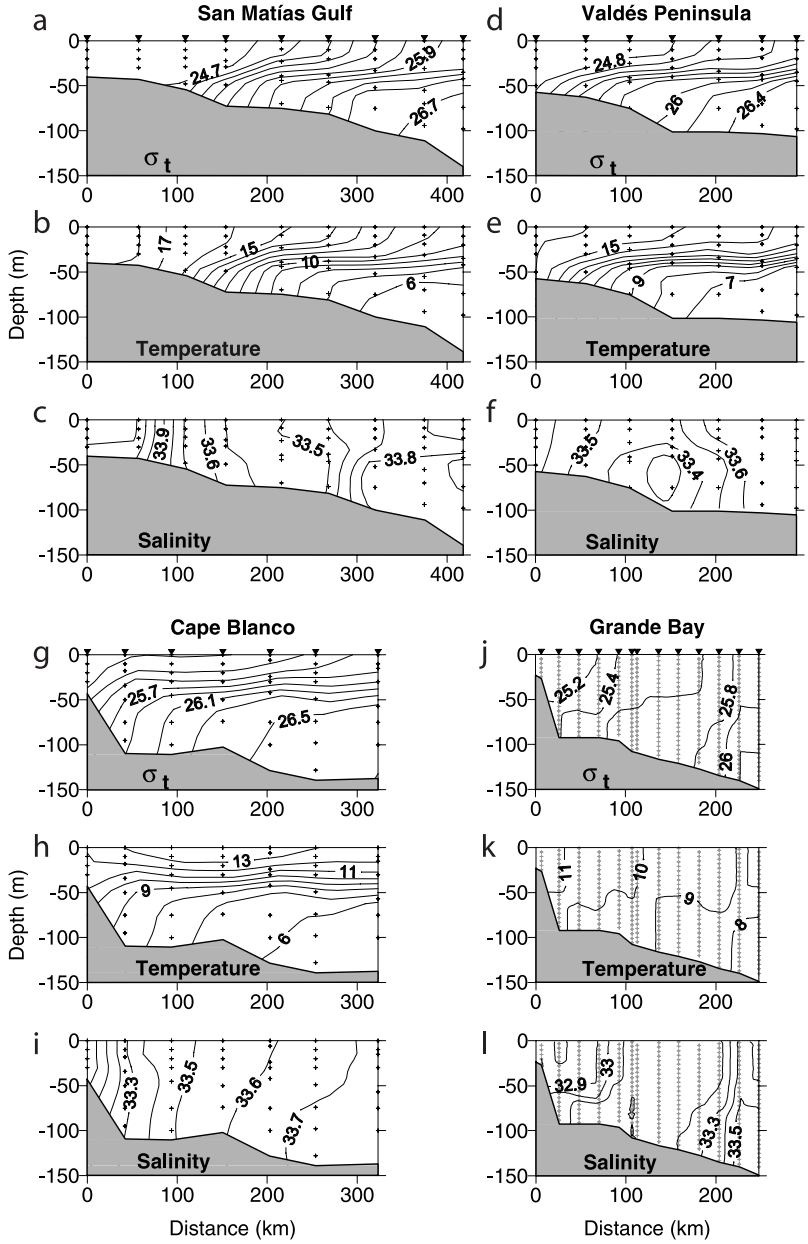

Figure 3. Vertical sections for (a–c) San Matías Gulf, (d–f) Valdés Peninsula, (g–i) Cape Blanco, and (j–l) Grande Bay transects, showing σ_t in kg m^{-3} (Figures 3a, 3d, 3g, and 3j), temperature in °C (Figures 3b, 3e, 3h, and 3k), and salinity (Figures 3c, 3f, 3i, and 3l). Isopycnals are shown every 0.2 kg m^{-3}, isotherms every 1°C and isohalines every 0.1.

the available transects, where the distance between stations is larger than the one appropriate to observe the frontal scale. Furthermore, the positive thermal anomalies of SMG can mask the cooler waters at the front of SMG. The first station of the VP transect is at the mouth of Nuevo Gulf where temperature warmer than offshore has been observed [*Rivas and Ripa*, 1989; *Rivas and Beier*, 1990].

[18] At SMG, coastal temperature and salinity (Table 2) are related to the circulation of the SMG which results in an outflow of warm and saline waters [*Piola and Scasso*, 1988]. In this vertical section (Figure 3), at about 340 km from the coast, near bottom high salinity (>33.8) and low temperature (<6°C) suggest mixing with Malvinas waters. Stratification at GB (Figure 3) is weaker than in other transects, throughout the entire section. This is due to the lower mixed layer temperature at higher latitudes. *Sabatini et al.* [2000], using recent hydrographic data from southern Patagonia, pointed out that south of 51°S the density structure of the water column is nearly homogeneous. Less stratified waters are apparent close to the easternmost station, which presents higher salinity and lower temperature than farther offshore, probably due to the influence of quasi-homogeneous waters of southern origin.

[19] Summarizing, from the inspection of the stratification along the selected transects, a division of the Patagonian continental shelf is formulated as follows:

[20] 1. The coastal region has quasi-homogeneous water and depths up to about 60 m.

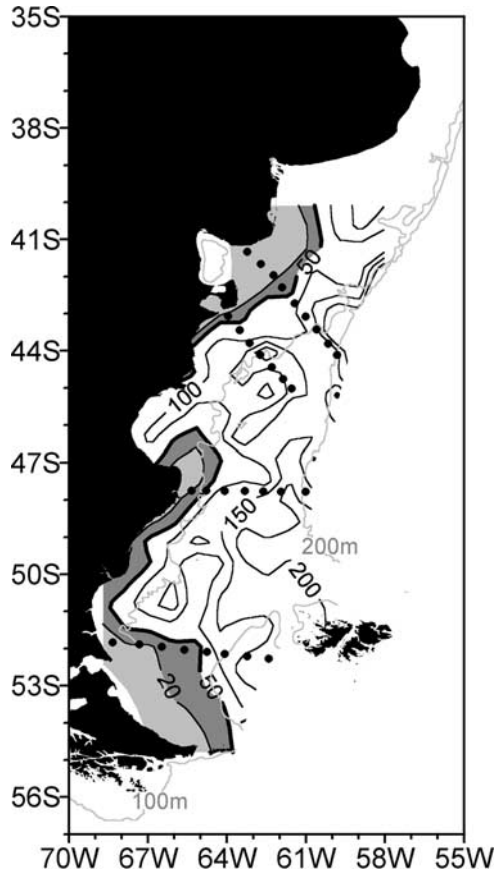

Figure 4. Simpson parameter (J m^{-3}) computed from summer hydrographic data. The bold line is the critical Simpson parameter (Φ_C = 50 J m^{-3}), shaded contours correspond to values $<\Phi_C$, and contour interval for values $>\Phi_C$ is 50 J m^{-3}. Dots show the four transects used to describe the tidal fronts.

[21] 2. The midshelf is where the thermocline is well developed and stratification reaches the highest values of the shelf (Table 2). The more stratified waters are located in the shelf area between 75 and 100 m isobaths. This region can be represented by two layers, with a ~20 m mixed layer separated from the near bottom layer by a strong thermocline.

[22] 3. The outer shelf is where stratification decays in the proximity of the shelf break.

3.2. Simpson Parameter

[23] To locate fronts on the continental shelf, the Simpson parameter Φ was computed using all available summer data. Since tidal fronts are boundaries between quasi-homogeneous and well-stratified waters, they are characterized by intermediate Simpson parameter values. After inspection of several vertical sections a value of Φ = 50 J m^{-3} was chosen to estimate the mean frontal position. Similar values (Φ = 40 J m^{-3}) have been used by *Sabatini et al.* [2000, 2004]. The Simpson parameter horizontal distribution in the shelf is presented in Figure 4.

[24] In the inner San Jorge Gulf, waters are stratified (values higher than 100 J m^{-3}) and present relatively high surface salinity and temperature (up to 33.6 and 17°C, respectively) compared to the midshelf. This can be observed by the position of the Φ = 50 J m^{-3} contour that intersects the coast at the northern tip of San Jorge Gulf and reappears in the area of CB. Between 51°S and 54°S, the area of well-mixed waters remarkably broadens, reaching the 150 m isobath at about 200 km from the coast (Figure 4) [see also *Sabatini et al.*, 2004].

3.3. Air-Sea CO_2 Fluxes

[25] The frontal scale (about 30 km) [*Bava et al.*, 2002] is not always well resolved by the transects because sometimes the ship track runs closely along the fronts. However, sharp changes in temperature and ΔpCO_2 across the tidal fronts are observed, i.e., close to VP and CB (Figure 5), in most midshelf transects. At VP, temperature rises from 14.7°C to 15.6°C, ΔpCO_2 drops from 60 to −90 μatm, while the fluorescence increases from 0.4 to 1.8 arbitrary units (a.u.), from the cold to the warm side of the front. Across the front at CB, temperature increases from 10.8°C to 13.4°C, ΔpCO_2 varies from 0 to −120 μatm, and the fluorescence rises from 1.9 to 2.8 a.u. The cross-front temperature increase is much larger at CB, while the ΔpCO_2 is slightly negative at the unstratified side of the front, and the ΔpCO_2 and fluorescence changes are larger at VP. Cold waters are associated with a well-mixed water column while the warmer waters are stratified. The high fluorescence in the stratified side of the front is probably linked to increased biological activity, which leads to the very low ΔpCO_2 (see also Chl *a* distribution in Figure 7).

[26] The ΔpCO_2 horizontal distribution in the study region is presented in Figure 6a. The areal mean ΔpCO_2 corresponding to the Patagonian shelf is −24 μatm and increases to approximately −29 μatm if the shelf break front is included. It can be observed that most of the continental shelf is a strong CO_2 sink area reaching values of ΔpCO_2 of −110 μtam (i.e., off San Jorge Gulf), among the strongest negative values in the global ocean [*Takahashi et al.*, 2002]. Historical nutrient data (not shown) present a relative maximum off San Jorge Gulf. Moreover, the fluorescence distribution pattern presents a maximum (Figure 5) at the stratified side of the front, probably due to a rapid uptake of nutrients in bloom events, which could cause the very low pCO_2 ocean values.

[27] The horizontal surface distribution of the sea-air CO_2 fluxes (Figure 6b) shows that while the coastal region acts as a source of CO_2 to the atmosphere, the midshelf and outer shelf are sinks, reaching fluxes of −55 mmol of CO_2 m^{-2} d^{-1}. The later fluxes correspond to values of ΔpCO_2 as low as −110 μatm. Only one cruise carried out in 2004 sampled the shelf break region, where the highest CO_2 fluxes into the ocean were recorded (−65 mmol of CO_2 m^{-2} d^{-1}). On the other hand, positive ΔpCO_2 with peaks that exceed 80 μatm, leading to fluxes >40 mmol m^{-2} d^{-1}, are found northeast of SMG front and east of GB front. The area (~800,000 km^2) averaged CO_2 flux over the continental shelf is −4.4 mmol m^{-2} d^{-1} and increases to −5.7 mmol m^{-2} d^{-1} if the shelf break front is included. The transition between positive and negative CO_2 fluxes closely follows the critical Simpson parameter isoline (50 J m^{-3}) suggesting a link between changes in vertical stratification and the regional dynamics of CO_2 fluxes. Although the Simpson parameter and ΔpCO_2 are not based on the same data sets, throughout the region the climatological values are negatively correlated (r^2 = 0.38) at a 99% confidence level. In

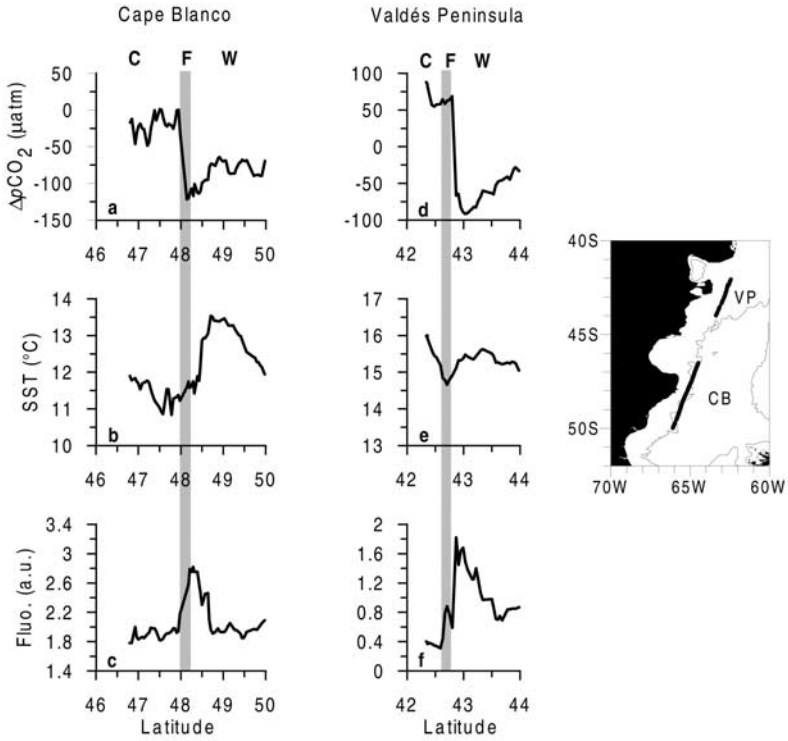

Figure 5. ΔpCO_2, SST, and fluorescence versus latitude for (a–c) Cape Blanco and (d–f) Valdés Peninsula fronts. Cold (well-mixed) and warm (stratified) regions are identified by C and W, respectively. The shaded area corresponds to the front (F), identified as the region between Simpson parameter values of 40 and 60 J m^{-3}. The inset shows the transects used to build the latitudinal series for Cape Blanco (25–26 January 2001) and Valdés Peninsula (10 April 2002).

addition, an increase in biological activity at the stratified side of the front can reinforce the sink of CO_2 to the ocean. The dissolved oxygen was sampled with a low spatial resolution, and it is therefore not shown. The surface distribution presents supersaturation (110%) in the midshelf and slight undersaturation (95%) in the tidal front coastal regions, further suggesting interaction of biological activity and the physical structure of tidal fronts.

[28] To analyze the influence of biology in the air-sea CO_2 fluxes, the Chl *a* horizontal distribution obtained from the discrete samples along the transects is shown in Figure 7. Although these samples have lower spatial resolution than the underway data, variations of Chl *a* across the above described fronts can be observed. At VP Chl *a* values increased from 0.7 mg m^{-3} at the homogeneous side of the front to >2 mg m^{-3} at the stratified side. A remarkable variation is evident at CB, where maximum Chl *a* values are usually present, averaging close to 3 mg m^{-3} Chl *a* at the stratified side of the front, contrasting with much lower values in the vicinities of the well-mixed coastal waters. Similarly, high Chl *a* is found north of San Jorge Gulf, with maximum Chl *a* (>2 mg m^{-3}) and at GB (3 mg m^{-3}). A Chl *a* maximum, not associated with tidal fronts, is observed at the shelf break front from 47°S to 50°S.

4. Discussion

[29] Previous works on the tidal fronts in the Patagonian shelf have shown that the abundance of certain plankton species, mainly diatoms [*Balech*, 1964, 1965] and dinoflagellates [*Carreto et al.*, 1981, 1986] is related with stratification. These studies have focused on relatively small frontal areas. The present work further discusses the physical structure of the tidal fronts and the contrasting environmental features of coastal and outer shelf waters on a regional scale.

[30] The CO_2 data set presented here is the first available in the Patagonian continental shelf. In the coastal region the location of tidal fronts closely matches the transition between positive and negative ΔpCO_2 regions. The ΔpCO_2 transition across the front can be a result of physical, biological, and combined physical-biological processes. Physical processes include the dissipation of the tidal energy, by means of bottom friction, which vertically mixes the water column leading to enhanced mixing and homogenization of CO_2. Because the CO_2 concentration generally increases with depth because of demineralization of dissolved organic matter [*Broecker and Peng*, 1982], the surface CO_2 will increase in the mixed side of the tidal front. In addition, since convection governs the vertical displacements of phytoplankton, intense vertical mixing may remove planktonic algae from the euphotic layer, inhibiting their growth and biological consumption of CO_2. *Carreto et al.* [1986] reported the presence of typically benthic diatom species and resting cysts of *Gonyaulax excavata* in the near-coastal zone off VP that are absent in the stratified side of the front and other tidal fronts (i.e., CB, J. I. Carreto, personal communication, 2003). Biological processes would include the addition of CO_2 to the water column by means of the respiration of benthic organisms in

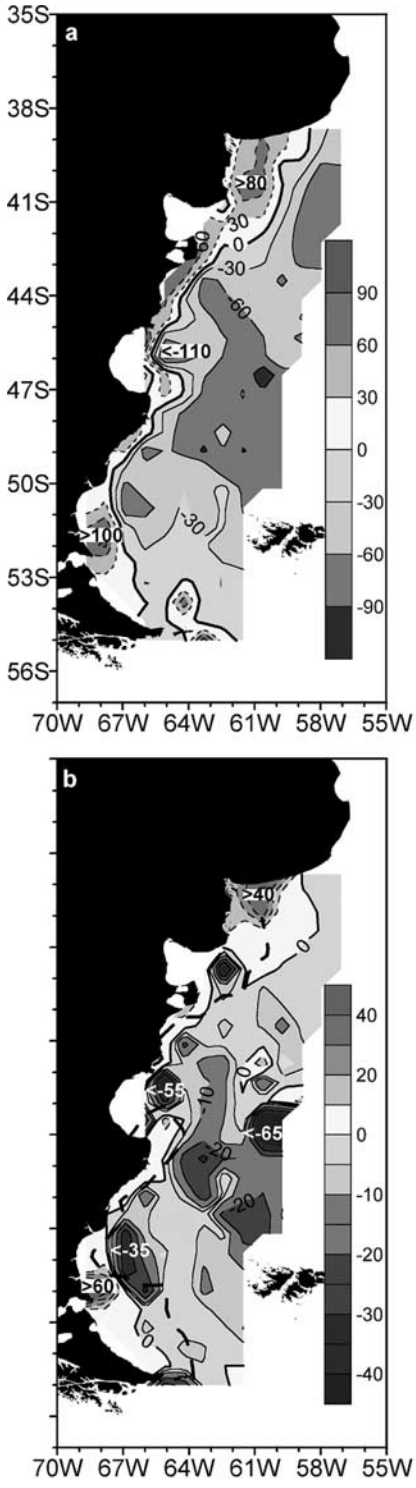

Figure 6. (a) Surface distribution of ΔpCO_2 (μatm). The bold line is the ΔpCO_2 zero value (contours every 30 μatm). Positive and negative values are east and west of the bold line, respectively. (b) Surface distribution of air-sea CO_2 fluxes. The critical Simpson parameter is represented by the dashed bold line. See color version of this figure at back of this issue.

the onshore side of the tidal front. The source of the organic matter respired by these organisms, like in other coastal heterotrophic environments [*Duarte and Agustí*, 1998], must be at least in part allochtonous, from land-derived organic carbon sources. In addition, cross-front exchanges are also a possible source of particulated and dissolved organic matter to the coastal region. Note that the offshore upper layers are isopycnally connected to the inshore lower layers providing a possible pathway for tracer exchange (see Figure 3).

[31] During summer and fall, east of the tidal fronts the midshelf region is a strong CO_2 sink (-4.4 mmol m^{-2} d^{-1}). The shelf break increases the mean absorption rate to -5.7 mmol m^{-2} d^{-1}, but only one cruise sampled this area in late Austral summer 2004. The mean is virtually identical when the CO_2 fluxes are calculated with the quadratic parameterization from W92: -4.6 mmol m^{-2} d^{-1} and -5.7 mmol m^{-2} d^{-1} if the shelf break region is included. Similar results have been obtained by *Hales et al.* [2005] off the Oregon coast in summertime. They found that surface water over most of the shelf was a strong sink for atmospheric CO_2, while a near-shore strip was an intense source. Similarly, *Thomas et al.* [2004] found that during summer in the North Sea the ΔpCO_2 distribution shows clear differences between stratified (northern) and nonstratified (southern) regions. As in the present work, the stratified area in the North Sea is strongly CO_2 undersaturated (up to -150 ppm), while the homogeneous area is supersaturated (up to 100 ppm). Though the data reveal that overall, the midshelf region is a CO_2 sink (approximately -10 mmol m^{-2} d^{-1}), the magnitude of the CO_2 flux increases significantly (less than -30 mmol m^{-2} d^{-1}) at the Chl *a* maxima (see Figure 6b), suggesting a modulation of the CO_2 fluxes by biological activity.

[32] The CO_2 fluxes estimated at GB are -45 mmol m^{-2} d^{-1} using the W92 parameterization and -35 mmol m^{-2} d^{-1} using WMG99. At the shelf break the flux difference is the largest: -50 mmol m^{-2} d^{-1} using W92 and -65 mmol m^{-2} d^{-1} using WMG99. However, typically CO_2 flux differences between estimates based on the two gas transfer velocity parameterizations are within ±5 mmol m^{-2} d^{-1}.

[33] Extrapolation of the overall shelf air-sea CO_2 flux to a whole year is not straightforward. Stratification in winter is removed by heat lost to the atmosphere and wind mixing [*Rivas and Piola*, 2002], and the incoming solar radiation is weaker than in summer and fall. Both effects must decrease photosynthesis and primary production. In the inner shelf the mean air pCO_2 difference between summer and winter is less than 1 μatm, which is the standard error of measurement. On the other hand, cooler surface water increases the solubility, and this will enhance sequestration of CO_2 from the atmosphere. The winter SST decrease over the Patagonian shelf is >3°C [*Bianchi et al.*, 1982]. At typical Patagonian shelf temperatures a decrease of 1°C leads to a seawater pCO_2 decrease of more than 10 μatm, leading to enhanced sequestration in winter. Furthermore, since the time for equilibration of the CO_2 system with the atmosphere is long (~1 year) compared to the time for thermal equilibration of the mixed layer (a few months), the thermal CO_2 signal may remain measurable even after the thermal forcing has ceased [*Watson and Orr*, 2002]. Consequently, opposed effects will affect the pCO_2 over the shelf, but the lack of

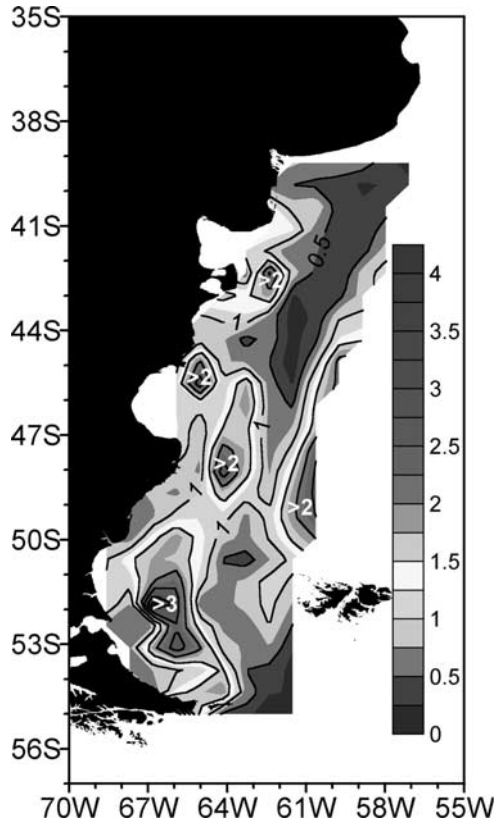

Figure 7. Surface distribution of Chl *a* (mg m^{-3}). Contour lines are every 0.5 mg m^{-3}. Note high values (>2 mg m^{-3}) offshore Valdés Peninsula, north and south of San Jorge Gulf and Grande Bay, related to the stratified side of tidal fronts. See color version of this figure at back of this issue.

observations during winter precludes the extrapolation of CO_2 yearly fluxes.

[34] The largest CO_2 source to the atmosphere (60 mmol m^{-2} d^{-1}) is observed inshore of the GB front. In this region the coastal surface cyclonic circulation may enhance primary production by favoring nutrient trapping [*Sabatini et al.*, 2004]. However, the input of deeper CO_2 rich waters to the sea surface will also increase the pCO_2. Thereby, the food availability leads to a "hot spot" of accumulation of zooplankton biomass (with peaks of up to 3500 mg m^{-3}, wet weight) observed from 1994 to 2000 during summer [*Sabatini et al.*, 2004]. The respiration of zooplankton and the increase of CO_2 by convection in this area would explain the maximum CO_2 flux to the atmosphere (Figure 6b).

[35] Studies carried out in the East China Sea have shown that the CO_2 uptake, and export to subsurface layers in the open ocean, may strongly enhance the absorption of CO_2 in continental shelves [*Tsunogai et al.*, 1999]. Because throughout the year the Patagonian shelf is occupied by waters less dense that the neighboring Malvinas Current, the so-called continental shelf pump cannot work in this region. The sense of the cross-shelf circulation in the Patagonian shelf is likely opposed to that of the East China Sea, with export of high CO_2 concentration shelf waters in the upper layer and input of open ocean waters in a subsurface layer. Such circulation scheme is supported by high-resolution numerical simulations [*Palma et al.*, 2004].

[36] Phytoplankton blooms generally occur in relatively small spatial scales and are short-lived. As the Argau data were collected in relatively short time intervals (typically 3 days) in the period from 2000 to 2004, it may be argued that they may not adequately display the mean summer-fall situation. However, the historical hydrographic data collected during several decades reveal changes in vertical stratification that closely match the transitions between positive and negative CO_2 fluxes and are also associated with sharp changes in fluorescence and Chl *a* as observed during the Argau experiment. This observation suggests that the Argau data are representative of the mean summer-fall conditions. Reports of high satellite-derived Chl *a* at VP, CB, and GB [*Acha et al.*, 2004], where we observed the largest atmospheric CO_2 sinks, provide independent evidence indicating that tidal fronts play a significant role in shaping the sea-air CO_2 fluxes. Though the satellite imagery presents significant interannual variability, during the summer, relatively high-Chl *a* regions are always evident at the location of tidal fronts (S. I. Romero, personal communication, 2005). Thus the summer and fall CO_2 flux structure associated with spatial changes in vertical stratification appears to be a semipermanent feature of the Patagonian shelf.

[37] **Acknowledgments.** The ARGAU Project is supported by Servicio de Hidrografía Naval, Instituto Antártico Argentino (IAA), Institut National de Sciences de l'Univers, Processus Biogeochimiques dans L'Ocean et Flux, Université Pierre et Marie Curie, the Inter-American Institute for Global Change Research Cooperative Research Network (CRN61), and the program ECOS-SECyT (A99U02). Additional financial support was provided by Universidad de Buenos Aires (UBACyT EX/002) and Agencia Nacional de Promoción Científica y Tecnológica (PICT99–0706420). QuikScat winds are produced by Remote Sensing Systems (RSS) and are supported by NASA Ocean Vector Winds Science Team. We are greatly indebted to the crew of the Icebreaker Almirante Irizar and scientists and technicians of the Argau Project. We thank Marcela Charo and Silvia Romero for scientific discussions and Alejandro Ulrich, Leonardo Cantoni, and Héctor Ochoa for technical support. Comments from the reviewers significantly improved the manuscript.

References

Acha, E. M., H. W. Mianzan, R. A. Guerrero, M. Favero, and J. Bava (2004), Marine fronts in the continental shelves of austral South America: Physical and ecological processes, *J. Mar. Syst.*, *44*, 83–105.

Bakun, A. (1993), The California current, Benguela current, and southwestern Atlantic shelf ecosystems: A comparative approach to identifying factors regulating biomass yields, in *Large Marine Ecosystems: Stress, Mitigation, and Sustainability*, edited by K. Sherman, L. M. Alexander, and B. D. Gold, pp. 199–221, AAAS, Washington, D. C.

Bakun, A., and R. H. Parrish (1991), Comparative studies of coastal pelagic fish reproductive habitats: The anchovy (Engraulis anchoita) of the southwestern Atlantic, ICES, *J. Mar. Sci.*, *48*, 343–361.

Balech, E. (1964), Fitoplancton de Mar del Plata durante el período 1961–1962, *Bol. Inst. Biol. Mar.*, *4*, 1–49.

Balech, E. (1965), Nuevas contribuciones a los esquemas de circulación oceánica frente a la Argentina, *An. Acad. Bras. Cienc.*, *37*, 157–166.

Bava, J., D. A. Gagliardini, A. I. Dogliotti, and C. A. Lasta (2002), Annual distribution and variability of remotely sensed sea surface temperature fronts in the Southwestern Atlantic Ocean, paper presented at 29th International Symposium on Remote Sensing of the Environment, Int. Cent. for Remote Sens. of Environ., Buenos Aires, Argentina.

Behrenfeld, M. J., and P. G. Falkowski (1997), A consumer's guide to phytoplankton Primary productivity models, *Limnol. Oceanogr.*, *42*(7), 1479–1491.

Bianchi, A. A., M. Massonneau, and R. M. Olivera (1982), Análisis estadístico de las características T-S del sector austral de la plataforma continental argentina, *Acta Oceanogr. Argent.*, *3*(1), 93–118.

Bisbal, G. (1995), The southeast South American shelf large marine ecosystem: Evolution and components, *Mar. Policy*, *19*, 21–38.
Broecker, W. S., and T.-H. Peng (1982), *Tracers in the Sea*, 690 pp., Lamont-Doherty Earth Obs., Palisades, New York.
Carreto, J. I., M. L. Lasta, R. M. Negri, and H. R. Benavides (1981), Los fenómenos de marea roja y toxicidad de moluscos bivalvos en el Mar Argentino, 55 pp., *Contrib. 399*, Inst. Nac. Invest. Desarollo Pesquero, Mar del Plata, Argentina.
Carreto, J. I., H. R. Benavides, R. M. Negri, and P. D. Glorioso (1986), Toxic red tide in the Argentine Sea. Phytoplankton distribution and survival of the toxic dinoflagellate Gonyaulax excavata in a frontal area, *J. Plankton Res.*, *8*, 15–28.
Carreto, J. I., V. A. Lutz, M. O. Carignan, A. D. Cucchi Coleoni, and S. G. De Marco (1995), Hydrography and chlorophyll-a in a transect from the coast to the shelf break in the Argentinian Sea, *Cont. Shelf Res.*, *14*, 315–336.
Codispoti, L. A., G. E. Friedrich, and D. W. Hood (1986), Variability in the inorganic carbon system over the southeastern Bering Sea shelf during spring 1980 and spring-summer 1981, *Cont. Shelf Res.*, *5*, 133–160.
Copin-Montégut, C. (1985), A method for the continuous determination of the partial pressure of carbon dioxide in the upper ocean, *Mar. Chem.*, *17*, 13–21.
Copin-Montégut, G. (1996), *Chimie de l'Eau de Mer*, 319 pp., Inst. Oceanogr. de Paris, Paris.
Duarte, C. M., and S. Agustí (1998), The CO_2 balance of unproductive aquatic ecosystems, *Science*, *28*, 234–236.
Frankignoulle, M., and A. V. Borges (2001), European continental shelf as a significant sink for atmospheric carbon dioxide, *Global Biogechem. Cycles*, *15*(3), 569–576.
Glorioso, P. D. (1987), Temperature distribution related to shelf-sea fronts on the Patagonian Shelf, *Cont. Shelf Res.*, *7*, 27–34.
Glorioso, P. D., and R. A. Flather (1997), The Patagonian Shelf tides, *Prog. Oceanogr.*, *40*, 263–283.
Guerrero, R. A., and A. R. Piola (1997), Masas de agua en la plataforma continental, in *El Mar Argentino y sus Recursos Pesqueros, Antecedentes Históricos de las Exploraciones en el Mar y las Características Ambientales*, vol. 1, edited by E. E. Boschi, pp. 107–118, Inst. Nac. Invest. Desarollo Pesquero, Mar del Plata, Argentina.
Hales, B., T. Takahashi, and L. Bandstra (2005), Atmospheric CO_2 uptake by a coastal upwelling system, *Global Biogeochem. Cycles*, *19*, GB1009, doi:10.1029/2004GB002295.
Hart, T. J. (1946), Report on trawling survey of the Patagonian continental shelf, *Discovery Rep.*, *23*, 223–248.
Hoskins, B. J., and F. B. Bretherton (1972), Atmospheric frontogenesis models: Mathematical formulation and solution, *J. Atmos. Sci.*, *29*, 11–37.
Kantha, L. H., C. Tierney, J. W. Lopez, S. D. Desai, M. E. Parke, and L. Drexler (1995), Barotropic tides in the global ocean from a nonlinear tidal model assimilating altimetric tides: 2. Altimetric and geophysical implications, *J. Geophys. Res.*, *100*, 25,309–25,317.
Krepper, C. M., and A. A. Bianchi (1982), Balance del Mar Epicontinental Argentino, *Acta Oceanogr. Argent.*, *3*(1), 119–133.
Lusquiños, A. J. (1971a), Algunas características de las aguas de la plataforma continental argentina, in *Datos y Resultados de las Campañas Pesquería, Pesquería X*, *Ser. Inf. Tec., Publ. 10/X*, edited by S. F. Villanueva, Proyecto de Desarrollo Pesquero, Mar del Plata, Argentina.
Lusquiños, A. J. (1971b), Algunas características de las aguas de la plataforma continental argentina, in *Datos y Resultados de las Campañas Pesquería, Pesquería XI*, *Ser. Inf. Tec., Publ. 10/XI*, edited by S. F. Villanueva, Proyecto de Desarrollo Pesquero, Mar del Plata, Argentina.
Lusquiños, A. J., and A. J. Valdés (1971), Aportes al conocimiento de las masas de agua del Atlántico Sudoccidental, *Rep. H659*, 48 pp., Serv. de Hidrografía Nav., Buenos Aires, Argentina.
Martos, P., and M. C. Piccolo (1988), Hidrography of the Argentine Continental Shelf between 38°S and 42°S, *Cont. Shelf Res.*, *8*, 1043–1056.
Metzl, N., A. Poisson, F. Louanchi, C. Brunet, B. Schauer, and B. Bres (1995), Spatio-temporal distributions of air-sea fluxes of CO_2 in the Indian and Antarctic oceans. A first step, *Tellus, Ser. B.*, *47*, 56–60.
Olson, D. B. (2002), Biophysical dynamics of ocean fronts, in *The Sea*, vol. 12, edited by A. R. Robinson, pp. 187–218, John Wiley, Hoboken, N. J.
Palma, E. D., R. P. Matano, and A. R. Piola (2004), Three dimensional barotropic response of the southwestern Atlantic shelf circulation to tidal and wind forcing, *J. Geophys. Res.*, *109*, C08014, doi:10.1029/2004JC002315.
Parker, G., M. C. Paterlini, and R. A. Violante (1997), El fondo marino, in *El Mar Argentino y sus Recursos Pesqueros, Antecedentes Históricos de las Exploraciones en el Mar y las Características Ambientales*, vol. 1, edited by E. E. Boschi, pp. 65–87, Inst. Nac. Invest. Desarollo Pesquero, Mar del Plata, Argentina.
Piola, A. R., and A. L. Rivas (1997), Corrientes en la Plataforma Continental, in *El Mar Argentino y sus Recursos Pesqueros, Antecedentes Históricos de las Exploraciones en el Mar y las Características Ambientales*, vol. 1, edited by E. E. Boschi, pp. 119–132, Inst. Nac. Invest. Desarollo Pesquero, Mar del Plata, Argentina.
Piola, A. R., and L. M. L. Scasso (1988), Circulación en el Golfo San Matías, *Geoacta*, *15*(1), 33–51.
Piola, A., et al. (2001), Air-sea CO_2 fluxes in the Southwest Atlantic ocean and the Patagonian shelf, paper presented at IAPSO/IABO Joint Assembly, Int. Assoc. for the Phys. Sci. of the Oceans and Int. Assoc. for Biol. Oceanogr., Mar del Plata, Argentina.
Poisson, A., N. Metzl, C. Brunet, B. Schauer, B. Bres, D. Ruiz Pino, and F. Louanchi (1993), Variability of sources and sinks of CO2 in the Western Indian and Southern oceans during the year 1991, *J. Geophys. Res.*, *22*, 759–778.
Quintana, F., and P. Yorio (1997), Breeding biology of Royal and Cayenne terns at a mixed species colony in Patagonia, *Wilson Bull.*, *109*, 650–662.
Rivas, A. L., and E. J. Beier (1990), Temperature and salinity fields in the north Patagonic gulfs, *Oceanol. Acta*, *13*, 15–20.
Rivas, A. L., and A. R. Piola (2002), Vertical stratification on the shelf off northern Patagonia, *Cont. Shelf Res.*, *22*, 1549–1558.
Rivas, A. L., and P. Ripa (1989), Variación estacional de la estructura termohalina de Golfo Nuevo, Argentina, *Geofís. Int.*, *28*(1), 3–24.
Sabatini, M. E., F. C. Ramírez, and P. Martos (2000), Distribution pattern and population structure of Calanus australis Brodsky, 1959 over the southern Patagonian Shelf off Argentina in summer, *ICES J. Mar. Sci.*, *57*, 1856–1866.
Sabatini, M. E., R. Reta, and R. Matano (2004), Circulation and zooplankton biomass distribution over the southern Patagonian shelf during late summer, *Cont. Shelf Res.*, *24*, 1359–1373.
Sarma, V. V. S. S. (2003), Monthly in surface pCO_2 and net air-sea CO_2 flux in the Arabian Sea, *J. Geophys. Res.*, *108*(C8), 3255, doi:10.1029/2001JC001062.
Scasso, L. M. L., and A. R. Piola (1988), Intercambio neto de agua entre el mar y la atmósfera en el Golfo San Matías, *Geoacta*, *15*(1), 13–31.
Simpson, J. H. (1981), The shelf-sea fronts: Implications of their existence and behaviour, *Philos. Trans. R. Soc. London Ser. A*, *302*, 531–546.
Simpson, J. H., and J. R. Hunter (1974), Fronts in the Irish Sea, *Nature*, *250*, 404–406.
Strickland, J. D. H., and T. R. Parsons (1972), A practical handbook of seaweater analysis, *Bull. 167*, 311 pp., Fish. Res. Board of Can., Ottawa, Ont., Canada.
Takahashi, T. (1961), Carbon dioxide in the Atmosphere and in Atlantic Ocean water, *J. Geophys. Res.*, *66*(2), 477–494.
Takahashi, T., et al. (2002), Global sea-air CO2 flux based on climatological surface ocean pCO_2 and seasonal biological and temperature effects, *Deep Sea Res. Part II*, *49*, 1601–1622.
Thomas, H., Y. Bozec, K. Elkalay, and H. J. W. de Baar (2004), Enhanced open ocean storage of CO_2 from shelf sea pumping, *Science*, *304*, 1005–1008.
Tsunogai, S., S. Watanabe, and T. Sato (1999), Is there a "continental shelf pump" for the absorption of atmospheric CO_2?, *Tellus, Ser. B*, *51*, 701–712.
Villanueva, S. F. (Ed.) (1968), *Datos y Resultados Preliminares de las Campañas Pesquería*, *Ser. Inf. Tec., Publ. 10/I–10/XIV*, Proyecto de Desarrollo Pesquero, Mar del Plata, Argentina.
Wanninkhof, R. (1992), Relationship between wind speed and gas exchange, *J. Geophys. Res.*, *97*, 7373–7382.
Wanninkhof, R., and W. R. McGillis (1999), A cubic relationship between air-sea CO2 exchange and wind speed, *Geophys. Res. Lett.*, *26*(13), 1889–1892.
Watson, A. J., and J. C. Orr (2002), Carbon dioxide fluxes in the global ocean, in Ocean Biogeochemistry: A JGOFS synthesis, edited by M. Fasham, J. Field, T. Platt, and B. Zeitzschel, pp. 123–141, Springer, Berlin, Germany.
Williams, P. J. (1990), Oceans, carbon and climate change, Scientific Committee on Oceanic Research (SCOR), Halifax, Canada.

C. F. Balestrini, A. A. Bianchi, and A. R. Piola, Departamento Oceanografía, Servicio de Hidrografía Naval, Av. Montes de Oca 2124, 1212 Ciudad de Buenos Aires, Argentina. (abianchi@hidro.gov.ar)
L. Bianucci, Departamento Ciencias de la Atmósfera y los Océanos, FCEN, Universidad de Buenos Aires, Ciudad Universitaria, Pabellón 2, 1428 Ciudad de Buenos Aires, Argentina.
D. R. Pino and A. Poisson, Laboratoire de Biogéochimie et Chimie Marines, Université Pierre et Marie Curie, 4 place Jussieu, F-75005 Paris, France.
I. Schloss, Instituto Antártico Argentino, Cerrito 1248, 1010 Ciudad de Buenos Aires, Argentina.

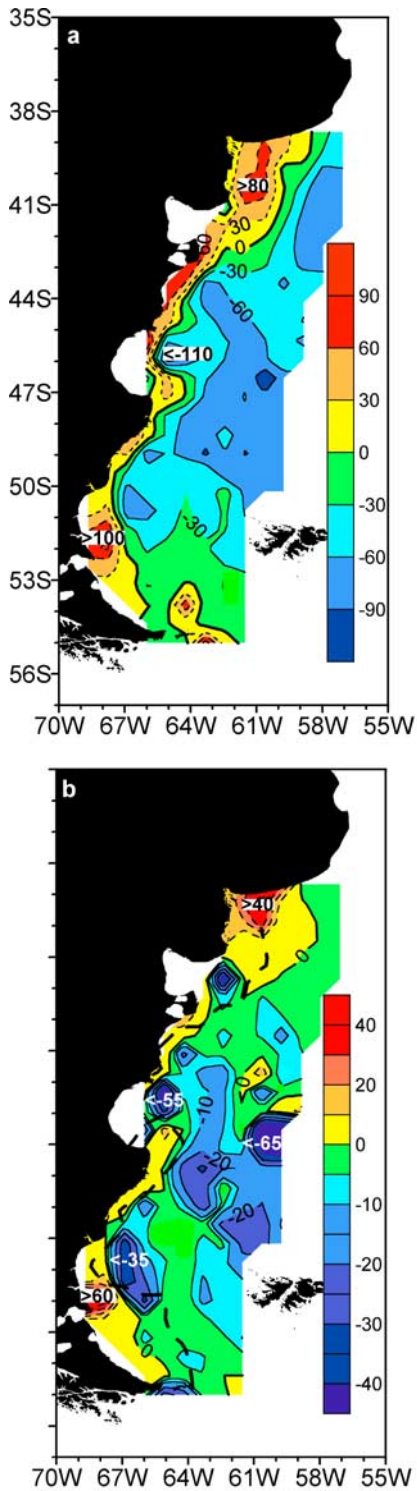

Figure 6. (a) Surface distribution of ΔpCO_2 (μatm). The bold line is the ΔpCO_2 zero value (contours every 30 μatm). Positive and negative values are east and west of the bold line, respectively. (b) Surface distribution of air-sea CO_2 fluxes. The critical Simpson parameter is represented by the dashed bold line.

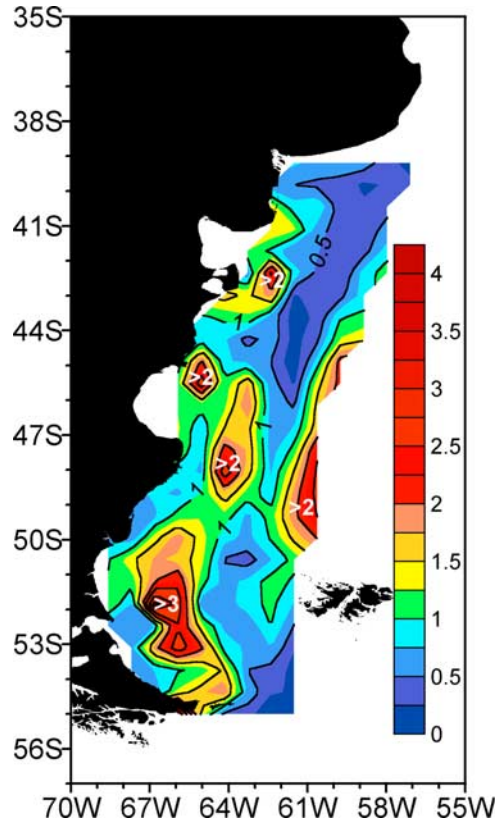

Figure 7. Surface distribution of Chl *a* (mg m^{-3}). Contour lines are every 0.5 mg m^{-3}. Note high values (>2 mg m^{-3}) offshore Valdés Peninsula, north and south of San Jorge Gulf and Grande Bay, related to the stratified side of tidal fronts.